Inorganic Chemistry

Article

pubs.acs.org/IC

Polytellurides of Mn, Fe, and Zn from Mild Solvothermal Reactions in Liquid Ammonia

Oleksandr Kysliak,[†] Max Marcus,[‡] Thomas Bredow,[‡] and Johannes Beck*[,†]

[†]Institut für Anorganische Chemie, Universität Bonn, Gerhard-Domagk-Strasse 1, 53121 Bonn, Germany

[‡]Mulliken Center für Theoretische Chemie, Universität Bonn, Beringstrasse 4, 53115 Bonn, Germany

Supporting Information

ABSTRACT: The reaction of elemental Mn, Fe, and Zn with Te in liquid ammonia at 50 °C leads to the polytellurides $[Mn(NH_3)_6]Te_4$ (**1**), $[Fe(NH_3)_6]$-$Te_4{\cdot}NH_3$ (**2**), and $[Zn(NH_3)_4]_2Te_{15}$ (**3**) in quantitative yield for **1** and **3**, and in 30−50% yield for **2**. The compounds form black crystals, which are air sensitive and easily lose ammonia without a protective atmosphere of NH_3. Compound **3** is semiconducting with a thermal activation energy of 1.2 eV. In the crystal structures of **1** and **2**, tetratelluride anions Te_4^{2-} in gauche conformation with dihedral angles around 90° are present, which are linked to form infinite spiral chains. Compound **3** contains an unusual Te_{15}^{4-} polyanion in the form of a bent chain Te_7−Te−Te_7. The connection between the Te_4 groups in **1** and **2** and the two Te_7 groups in **3** is achieved via linear Te_3 entities, which are strongly asymmetric in **1**, almost symmetric in **2**, and symmetric in **3** (for **1**, Te−Te···Te 174.0°, d_1 = 2.87, d_2 = 3.25 Å; for **2**, Te−Te−Te 178.8°, d_1 = 3.01, d_2 = 3.09 Å; for **3**, Te−Te−Te 180°, $d_1 = d_2$ = 3.06 Å). Periodic DFT calculations show that interaction between the Te_4^{2-} units is negligible in **1** and weak but undoubtedly present in **2**. The overlap population amounts to 0.09 in the linear Te_3 group of **3**. The band structure calculation of **3** gives semiconducting behavior with a band gap of 1.5 eV in fair agreement with experimental data.

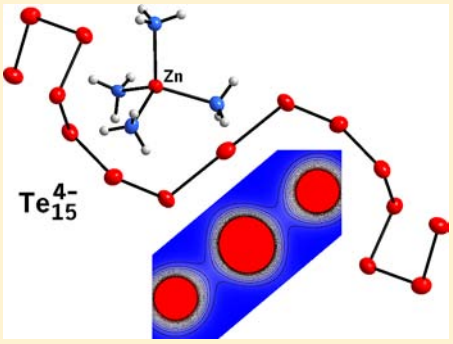

INTRODUCTION

Polytellurides show a large variability of Te−Te covalent and noncovalent interactions,[1] which makes the structural chemistry of these compounds interesting from a theoretical point of view. Tellurium-rich compounds find application as fast-ion conductors,[2] phase-change materials,[3] and thermoelectrics.[4] Therefore, syntheses as well as structural, theoretical, and physical studies of novel polytellurides are still in the focus of actual research work. According to the basic Zintl rules, a chalcogen polyanion is expected to contain single and 2-fold coordinated atoms in a ratio reflecting directly the overall charge of the ion. All atoms with coordination number two are formally neutral, and every singly coordinated chalcogen atom carries one negative charge. These simple rules are, however, often broken. For the heavier chalcogens, multicenter bonding is claimed to be responsible for more complicated structures. This holds especially for tellurium as a 5th period element. Higher coordination numbers beyond two are a generally observed structural feature in the structures of tellurium polyanions.

Common methods for the synthesis of polychalcogenides are high-temperature techniques, ammonothermal reactions, solvothermal reactions in CH_3OH and chelating amines at around 200 °C, or electrochemical syntheses.[5] Disadvantages of these methods are harsh reaction conditions or complicated experimental techniques.

Here we report a new "soft" synthetic way toward polytellurides of less-noble metals: low-temperature solvothermal synthesis in liquid ammonia from the elements. Although syntheses of metal chalcogenides in liquid ammonia at ambient temperatures have already been performed,[6] only the formation of binary phases with already known compositions was reported. In contrast, the new method allows for the synthesis of definite crystalline polytellurides with more complicated structures at temperatures slightly above room temperature.

Thick walled glass ampules can withstand the internal vapor pressure of liquid NH_3, allowing researchers to perform the ammonothermal reactions with normal laboratory equipment.

EXPERIMENTAL SECTION

Caution: *Glass ampules filled with liquid ammonia contain a high internal pressure, especially when heated. Heating may be performed only with precautions against injuries in case of explosion.*

Materials and Instruments. EDX measurements were performed with a scanning electron microscope/energy dispersive X-ray analyzer DSM 940 (Zeiss)/Genesis 2000 (Ametek). Conductivity measurements were performed by the two probe technique on compressed pellets. TG-DTA analyses were performed using a thermoanalyzer STA429 (Netzsch), and ICP analyses were performed after dissolution of the samples in nitric acid using an IRIS Avantage OES (Thermo Jarrel Ash).

General Synthetic Procedures and Materials. All chemicals (powdered zinc, manganese, iron, and tellurium, $MnCl_2$, $FeCl_2{\cdot}4H_2O$, $ZnCl_2$, ammonia) were commercially available and used without

Received: November 15, 2012
Published: July 12, 2013

   dx.doi.org/10.1021/ic302503u | Inorg. Chem. 2013, 52, 8327−8333

additional pretreatment. For the syntheses, thick walled glass ampules (inner diameter 5 mm, wall thickness 3.5 mm, length 6−8 cm) carrying a glass joint were used. The ampules were loaded with the respective metal powder, Te powder, and metal dichloride. With the use of a gas torch the glass tube in the upper part of the ampule was heated and on softening of the glass drawn to a thin capillary. The as-prepared ampule was then connected to a combined vacuum/NH_3 line. After evacuation, gaseous NH_3 was allowed to enter. External cooling of the ampule with liquid nitrogen caused the ammonia to freeze inside the ampule. After a sufficient amount of NH_3 had condensed, the ampule was closed by melting at the tapering position using a gas torch. This technique ensures the pressure resistance of the ampules since a sufficient wall thickness at the closing tip is assured. Heating was performed in an oven with the ampule in horizontal position. To isolate the product after the reactions, the content of the ampules was frozen with liquid nitrogen, and after scoring by a glass-cutter, the ampules were broken manually and the crystals poured into perfluorinated oil.

$[Mn(NH_3)_6]Te_4$ (1). Mn (7 mg, 0.125 mmol), Te (64 mg, 0.5 mmol), and $MnCl_2$ (21 mg, 0.17 mmol) were heated in liquid ammonia (0.3−0.5 mL) at 50 °C for 4 weeks. Compound **1** precipitates as black crystals with metallic luster in virtually quantitative yield.

$[Fe(NH_3)_6]Te_4{\cdot}NH_3$ (2). Fe (7 mg, 0.125 mmol), Te (64 mg, 0.5 mmol), and $FeCl_2{\cdot}4H_2O$ (33 mg, 0.17 mmol) were heated in liquid ammonia (0.3−0.5 mL) at 50 °C for 4 weeks. Compound **2** forms black crystals, which were obtained in 30−50% yield.

$[Zn(NH_3)_4]_2Te_{15}$ (3). Zn (22 mg, 0.33 mmol), Te (320 mg, 2.5 mmol), and $ZnCl_2$ (23 mg, 0,17 mmol) were heated in liquid ammonia (0.3−0.5 mL) at 50 °C for 2 weeks. Black crystals of **3** in millimeter size are formed in virtually quantitative yield.

Crystal Structure Determinations. Crystals of **1**, **2**, and **3** are sensitive toward the loss of ammonia and sufficiently stable at room temperature for a short time but only when protected from air. Therefore single crystals were selected while covered with perfluorinated oil at ambient temperature and then transferred into the cold nitrogen stream of the crystal cooling device of a Bruker-Nonius Kappa-CCD diffractometer equipped with graphite monochromatized Mo Kα radiation. Data collections were performed at −150(2) °C (123(2) K). Crystal systems, lattice types, and the space groups were derived from simulated precession photographs. The crystal structures were solved by direct methods[7] and refined on the basis of full-matrix least-squares on F^2 with the SHELX-97 program suite.[8] An analytical absorption correction was applied for **1** and **2** while multiscan absorption correction was performed for **3**. All non-hydrogen atoms were refined with anisotropic displacement coefficients. The hydrogen atoms of the NH_3 groups were placed in geometrically calculated positions and refined using constraints. X-ray crystallographic data and refinement details for all compounds are summarized in Table 1. Further details of the crystal structure investigations may be obtained from Fachinformationszentrum Karlsruhe, Germany (crysdata@fiz-karlsruhe.de), on quoting the CSD numbers CSD-425410 for **1**, CSD-425409 for **2**, and CSD-425411 for **3**.

RESULTS AND DISCUSSION

Synthesis and Properties. At temperatures slightly above room temperature, liquid ammonia turned out to be a suitable solvent for the synthesis of metal polytellurides. Metals with low oxidation potentials are oxidized by elemental tellurium under mild conditions and form the respective ammine complexes. So far, the reactions succeeded with Zn, Mn, and Fe, leading to the cationic complexes $[Zn(NH_3)_4]^{2+}$, $[Mn(NH_3)_6]^{2+}$, and $[Fe(NH_3)_6]^{2+}$ with elemental tellurium converted into different kinds of polytelluride anions. $[Mn(NH_3)_6]Te_4$ (**1**), $[Fe(NH_3)_6]Te_4{\cdot}NH_3$ (**2**), and $[Zn(NH_3)_4]_2Te_{15}$ (**3**) are selectively formed at 50 °C as pure phases and precipitate out of the solutions in almost quantitative yield for **1** and **3** and in 30−50% yield for **2**.

Table 1. Crystallograhic Data and Details of Structure Determination for $[Mn(NH_3)_6]Te_4$ (1), $[Fe(NH_3)_6]Te_4{\cdot}NH_3$ (2), and $[Zn(NH_3)_4]_2Te_{15}$ (3)

	1	2	3
formula	$H_{18}MnN_6Te_4$	$H_{21}FeN_7Te_4$	$H_{24}N_8Te_{15}Zn_2$
M_r/g mol^{-1}	667.54	685.49	2181.02
space group	$P2_1/n$	$P2_1/c$	$P2_1/c$
a/Å	8.8101(1)	7.4165(1)	9.6837(6)
b/Å	18.0435(2)	14.9666(1)	12.7783(11)
c/Å	9.6930(1)	15.6257(1)	13.1960(8)
β/deg	97.968(1)	112.8500(4)	96.053(4)
V /Å^3	1525.97(3)	1598.34 (3)	1623.8(2)
Z	4	4	2
reflns ($I > 2\sigma(I)$)	5403	3376	6014
refined params	107	125	120
$R(F)/wR(F^2)$ ($F_o > 4\sigma(F_o)$)	0.034/0.065	0.022/0.052	0.027/0.048

The reaction rates mirror the different activities of the metals. With Zn, a complete conversion to the polytelluride is achieved within two weeks. Mn needs four weeks for a complete conversion, and for Fe even after this prolonged reaction time conversion is incomplete. The addition of the respective metal chlorides to the reaction mixture of metal and Te was found to be advantageous, as the reaction rates and the quality of crystals were enhanced. However, compounds **1**−**3** can also be obtained in absence of these salts. The reactions are not sensitive to maintaining the exact metal: tellurium ratio. Only by using a very large excess of one component, e.g., a 10-fold excess of Zn metal for **3** or by largely prolonged reaction times for **2** and **3**, are the black crystals of the initially formed polytellurides converted to unidentified gray powders. It was found that **1**, **2**, and **3** may also be synthesized using the respective metal monotelluride and elemental tellurium as starting compounds.

All three compounds are black and show different stabilities. Due to the incorporated ammonia, **2** is the most sensitive compound and decomposes immediately on exposure to air. Crystals of $[Fe(NH_3)_6]Te_4{\cdot}NH_3$ (**2**) can only be kept for a few hours outside the reaction ampule under in polyfluorinated oil due to easy loss of NH_3 and oxidation. EDX analysis of the residue left after decomposition shows Fe:Te = 1:3 atomic ratio, which is in agreement with the formula of **2** in the range of experimental error. Crystals of $[Mn(NH_3)_6]Te_4$ (**1**) can be kept for some weeks under a protective layer of perfluorinated oil, preserving them from decomposition. EDX analysis of the residue after decomposition in air gave a Mn:Te = 1:4 atomic ratio. The crystals of $[Zn(NH_3)_4]_2Te_{15}$ (**3**) are the most stable of the series and can be kept in air at room temperature for a few days, but they also slowly lose ammonia. Covered with polyfluorinated oil, the crystals of **3** are stable for some weeks. They are insoluble in and inert to water and can be washed with an aqueous solution of NH_3 (25%), ethanol, and acetone. On slight heating to 50 °C the crystals keep their shape, but the faces turn dull. EDX analysis of this residue gave a Zn:Te atomic ratio of 1:5.5. ICP analysis of undecomposed material gave Zn 5.2%, Te 90.7%; calcd Zn 6.0%, Te 87.8% (mass). Both results are in agreement with the formula of 3 in the range of experimental error.

Our experiments indicate that polytellurides of other 3d metals cannot be obtained by the proposed method. This may be explained either by the low stability of ammonia complexes

dx.doi.org/10.1021/ic302503u | Inorg. Chem. 2013, 52, 8327−8333

with metal in low oxidation state, or, on the other hand, by the high oxidation potential of some metals (Co, Ni, Cu), which make the reduction of Te impossible under the experimental conditions. The metal successfully used in this type of reactions must form sufficiently stable ammine complexes and have an oxidation potential low enough to react with the relatively weak oxidant elemental tellurium. So far, only Zn, Mn, and Fe match these criteria.

Crystal Structures. In the structure of $[Mn(NH_3)_6]Te_4$ (**1**), all atoms are located in general crystallographic positions (Figure 1). The space group was chosen in the non-standard setting $P2_1/n$ for the reason of a convenient monoclinic angle β. The structure of **1** is built of separated Te_4^{2-} anions with Te–Te distances within the chain in the range 2.7473(3)–2.8659(4) Å, indicating single covalent bonding. The Te_4 chain is in gauche conformation with a Te1–Te2–Te3–Te4 dihedral angle of 99.9°. Applying the basic valence rules, the charge "−1" is located on both terminal one-fold coordinated atoms Te1 and Te4. However, while Te1–Te2 and Te2–Te3 bond lengths are almost identical, Te3–Te4 is 11 pm longer, which may be caused by secondary Te···Te interactions in the structure. There is a relatively short noncovalent interaction Te1–Te4 with a distance of 3.2460(4) Å between neighboring Te_4^{2-} anions, which is comparable to those found in $[Mn(en)_3]Te_4$,[9] interpreted as forming infinite polyanionic chains. Longer Te···Te secondary interactions between the chains are observed in the structure of **1** with the distances 3.6069(3) and 3.6149(3) Å (Te3–Te3′ and Te2–Te2′, respectively). Taking into account all Te···Te covalent and noncovalent interactions shorter than the sum of van der Waals radii for two Te atoms (approximately 4.1 Å), compound **1** represents a 2D polymeric anion structure.

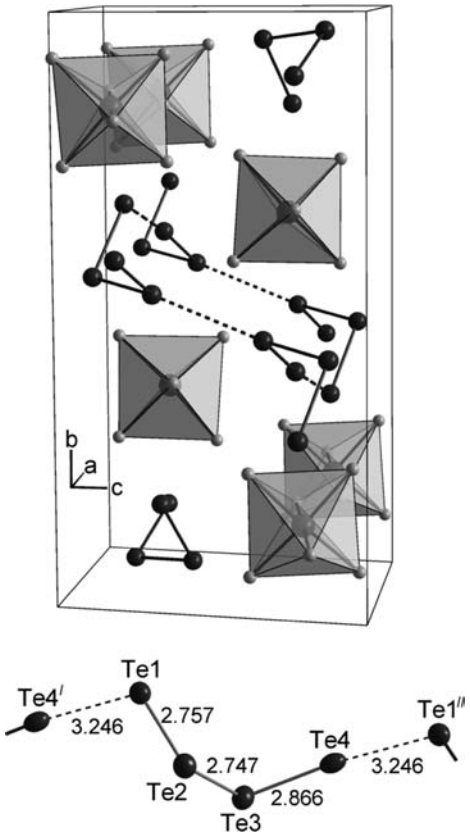

Figure 1. Unit cell of $[Mn(NH_3)_6]Te_4$ in a perspective view along the *a* axis (top) and a section of the $(Te_4^{2-})_n$ spiral chains (bottom). $[Mn(NH_3)_6]^{2+}$ ions are depicted as transparent octahedra, and hydrogen atoms are omitted. The broken lines indicate secondary Te–Te interactions between $(Te_4^{2-})_n$ strands. The Te–Te bond lengths are given in Å. Thermal ellipsoids are scaled to include a probability of 90%. Symmetry operators refer to I = −1 + *x*, *y*, *z*; II = 1 + *x*, *y*, *z*.

The cationic complex $[Mn(NH_3)_6]^{2+}$ shows a slightly distorted octahedral coordination of the central atom with Mn–N distances in the range 2.243(3)–2.319(4) Å. The so far structurally characterized $[Mn(NH_3)_6]^{2+}$ ions show Mn–N bonds in the same region between 2.25 and 2.31 Å.[10] The orientation of the NH_3 ligands implies some H-bonding interaction between cations and anions (shortest distance: d(Te···H) = 2.8439(2) Å with N–H···Te 160.2(2)°, d(N–Te) = 3.694(3) Å).

In the structure of $[Fe(NH_3)_6]Te_4{\cdot}NH_3$ (**2**) all atoms are located in general crystallographic positions. The unit cell contains analogous building units as the structure of **1**, i.e., octahedral $[Fe(NH_3)_6]^{2+}$ complexes and polytelluride anions. Additionally, discrete NH_3 solvate molecules are embedded in the unit cell (Figure 2). Like in the structure of **1**, the Te_4 chain takes a gauche conformation with a dihedral angle of 94.8°. Compound **2** is formally a tetratelluride, but the uniqueness of this compound is that it does not contain discrete, discriminable Te_4^{2-} anions. Instead, the individual Te_4 groups

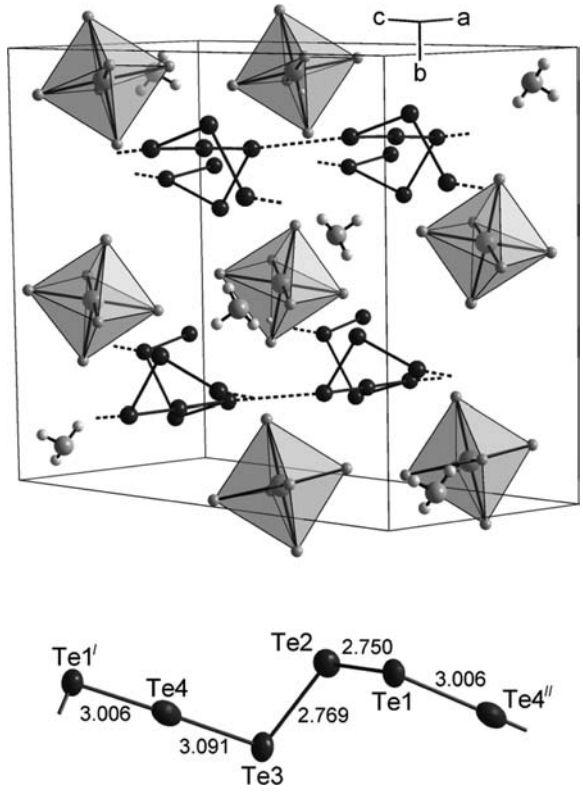

Figure 2. Unit cell of $[Fe(NH_3)_6]Te_4{\cdot}NH_3$ in a view along the [101] direction (top) and a section of the $(Te_4^{2-})_n$ spiral chain (bottom). $[Fe(NH_3)_6]^{2+}$ ions are depicted as transparent octahedra. The broken lines indicate secondary Te···Te interactions between $(Te_4^{2-})_n$ strands (3.606 Å). The Te–Te bond lengths are given in Å. Thermal ellipsoids are scaled to include a probability of 90%. Symmetry operators refer to I = 1 + *x*, 0.5 − *y*, 0.5 + *z*; II = −1 + *x*, 0.5 − *y*, −0.5 + *z*.

dx.doi.org/10.1021/ic302503u | *Inorg. Chem.* 2013, 52, 8327–8333

come in close contact and form 1D polymeric chains $(Te_4^{2-})_n$. Te−Te single bond lengths are observed for Te1−Te2 and Te2−Te3 (2.7501(3) and 2.7695(3) Å, respectively). The atoms Te4 are linearly coordinated with two almost equal bonds, Te3−Te4 with 3.0914(3) Å and Te1−Te4′ with 3.0063(3) Å. The bond lengths suggest three-center−four-electron bonds with a Te−Te bond order of 0.5 and the charge "−0.5" on Te3 and Te1 atoms and "−1" on Te4, respectively. The average Te−Te distance inside the polyanionic chain is 2.91 Å and is definitely longer than in elemental Te (average 2.83 Å), also indicating that the Te−Te bond order is in average less than 1. The shortest and only present secondary noncovalent interaction between the chains is Te1···Te3 with a distance of 3.6058(4) Å connecting the chains to a 2D layered motif.

The cation $[Fe(NH_3)_6]^{2+}$ shows a slightly distorted octahedral coordination of the central atom with Fe−N distances in the range 2.183(3)−2.240(2) Å with weak H-bonding interactions between cations and anions (shortest d(Te···H) = 2.8752(2) Å, angle N−H···Te 165.9(2)°, d(N···Te) = 3.745(3) Å). The $[Fe(NH_3)_6]^{2+}$ complex has only been rarely characterized.[11] The so far observed Fe−N bonds between 2.21 and 2.23 Å are in accordance with the Fe−N bond lengths found in the structure of **2**.

The comparison of the two closely related crystal structures of **1** and **2** shows as the predominant common feature the specific interaction between the tetratelluride chains. The Te_4^{2-} ions in both structures, in gauche conformation with dihedral angles close to 90°, are arranged to form infinite spiral chains. Formally, the Te atoms at the end of a polytelluride chain carry the negative charges. The bonding interaction outweighs the electrostatic repulsion. In both structures, an almost linear Te_3 fragment is present at the junction, which may be interpreted as multicenter bonding. In the structure of **1**, the Te_3 group is strongly asymmetric, while in the structure of **2** this group is almost symmetric, since the two Te−Te bonds differ by less than 0.1 Å. One-dimensional polymeric chains are a known feature in polytelluride chemistry and are found in the structures of other polytellurides such as In_2Te_5,[12] Tl_2Te_3,[13] $LiTe_3$,[14] Cs_2Te_5,[15] and Rb_2Te_5.[16] Secondary Te···Te interactions connect the polytelluride chains to 2D polyanionic layers, which was previously observed for tetratellurides only in the structure of $[TMDH]Te_4$.[17] This linking gives **1** and **2** similarities to other polytellurides like $ZrTe_3$[18] or $M^{I}Ln^{III}Te_4$.[19] It is worth noting that the homoleptic hexammine complexes $[Mn(NH_3)_6]^{2+}$ and $[Fe(NH_3)_6]^{2+}$ as present in **1** and **2** are rarely found and apparently formed only in liquid ammonia.[20]

The structure of $[Zn(NH_3)_4]_2Te_{15}$ (**3**) is dominated by a complicated and unprecedented polytellurium anion Te_{15}^{4-} (Figure 3). Related polytellurides with similar structural features are NaTe,[21] which contains a Te_5^{4-} anion, $[MTe_7]^{n-}$ anions,[22] and Ba_2SnTe_5.[23] However, the structure of **3** completely differs from the known polytellurides with Zn−amine complexes as cations.[24]

The interpretation of the structure of the polytelluride anion in **3** depends mainly on the limits up to which Te−Te bonding is considered. Several distances in the single bond region between 2.7567(4) and 2.8615(4) Å are present between the atoms Te1 and Te7. Te8 plays a special role. In contrast to the other Te atoms, it is located in an inversion center and linearly coordinated. The two respective bond lengths Te7−Te8 are equal and amount to 3.0606(3) Å. If Te−Te bonds up to 3.1 Å are considered, the overall structure of the Te_{15}^{4-} anion is a long

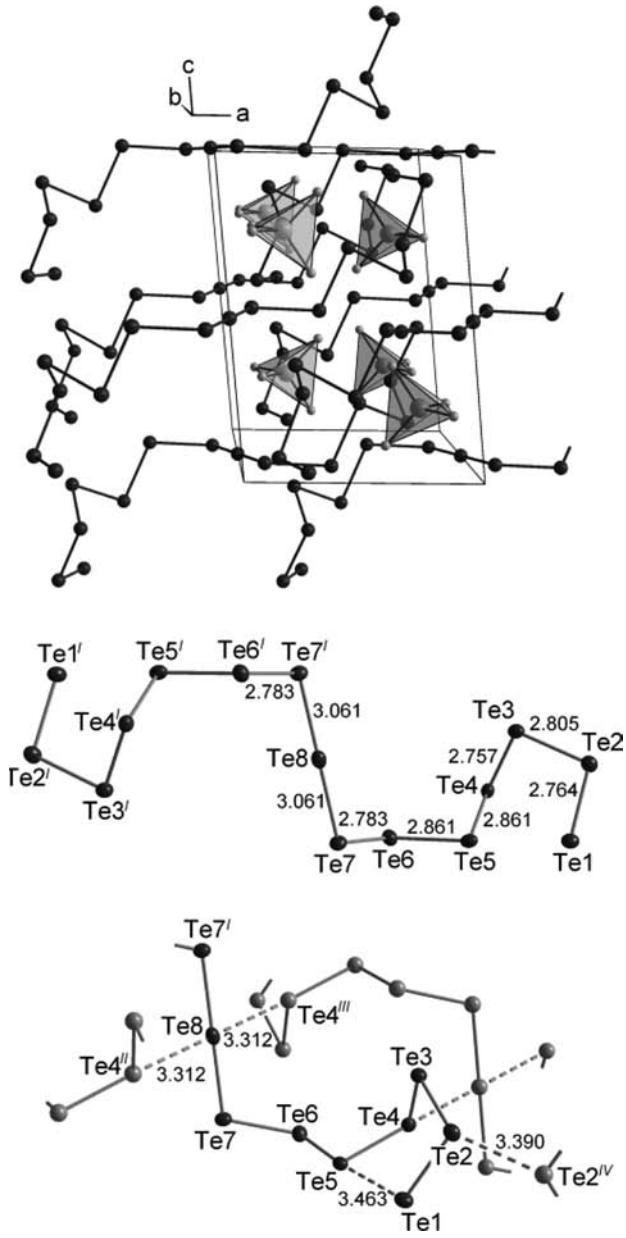

Figure 3. Unit cell of $[Zn(NH_3)_4]_2Te_{15}$ in a view along the b axis (top), the Te_{15}^{4-} anion (middle), and the connection of the Te_{15}^{4-} anions by secondary Te−Te interactions (broken lines, bottom). $[Zn(NH_3)_4]^{2+}$ ions are depicted as transparent tetrahedra. The Te−Te bond lengths are given in angstroms. Thermal ellipsoids are scaled to include a probability of 90%. Symmetry operators refer to I = $-x$, 1 - y, $-z$; II = $-1 + x$, y, z; III = $1 - x$, $1 - y$, $-z$; IV = $2 - x$, 1 - y, $1 - z$.

bent chain of 15 Te atoms. As in the structure of **2**, a three-center bond may be assumed with bond orders Te7−Te8/Te7′−Te8 of 0.5 and the charges "−1" on Te8, "−0.5" on both Te7 atoms, and "−1" located on both terminal atoms Te1 and Te1′, giving the overall charge of −4 for the chain in accordance with the valence rules. The average Te−Te distance within the Te_{15}^{4-} anion is 2.84 Å, which is slightly longer than in elemental Te, indicating that not all Te−Te bonds within the chain are single bonds.

There is a wide spectrum of additional secondary noncovalent Te···Te interactions in **3**, which are shorter than the sum of van der Waals radii for Te, and all Te atoms are involved in secondary bonding. The most interesting is the

dx.doi.org/10.1021/ic302503u | Inorg. Chem. 2013, 52, 8327−8333

Te8···Te4 interaction with a distance of 3.3121(3) Å. Te8 gains a distorted square planar coordination ($Te8(Te7)_2(Te4)_2$). The distance between Te1 and Te5 is 3.4626(4) Å, which leads to the formation of a five-membered Te_5 ring within the entire Te_{15} chain. Taking into account all secondary interactions with Te−Te distances up to 3.56 Å finally leads to a 3D polyanionic structure of connected Te atoms with large holes, in which the $[Zn(NH_3)_4]^{2+}$ cations are embedded.

The cationic complex $[Zn(NH_3)_4]^{2+}$ is of almost undistorted tetrahedral shape with Zn−N bond lengths in the range 2.010(3)−2.023(4) Å. $[Zn(NH_3)_4]^{2+}$ is a widely known complex.[25] The tetrahedral symmetry is generally barely distorted. Zn−N bonds are found between 1.99 and 2.05 Å, which is in line with the bonds found here. Weak hydrogen bonding between cations and anions is indicated by the Te···H distances (shortest d(Te···H) = 2.8101(3) Å, angle N−H···Te 173.2(2)°, d(Te···N) = 3.695(4) Å).

Physical Properties of $[Zn(NH_3)_4]_2Te_{15}$. As **3** is relatively stable at normal conditions, its thermal behavior and electrical conducting properties could be examined. TG-DTA (24−300 °C, 5 °C/min) analysis of **3** shows two steps of endothermic mass loss, 1.39% at 62.7 °C and 4.42% at 136.2 °C, adding up to a total mass loss of 5.81%. This can be straightforwardly interpreted as loss of ammonia in two steps of one molecule and three molecules of NH_3, respectively. The calculated mass of ammonia in **3** amounts to 6.24%. The only crystalline product after thermal decomposition is Te, as identified by X-ray powder diffraction. Measurement of electrical resistance against temperature for **3** in the interval 223−255 K shows exponentially decreasing resistivity (R) with the rise of temperature (T) (Figure S4a). The Arrhenius plot $\ln(R) = f(T^{-1})$ is linear, which is typical for semiconducting behavior (Figure S4b). From the slope of this function the activation energy for the thermal electron transport was obtained as 1.2 eV.

Electronic Structure Calculations. In order to analyze the bonding situation in the polytellurides the three systems were investigated theoretically at density functional theory (DFT) level. The hybrid functional PW1PW,[26] which has been successfully employed for the study of electronic properties of thianthrene hexafluorophosphate, was used.[27] All calculations were performed with the crystalline orbital program package CRYSTAL09.[28] The atomic basis sets were optimized in preliminary calculations for the monoammines of the metals with respect to the binding energies and geometries obtained from CCSD(T)/TZVP calculations by George et al.[29] An effective core potential combined with a 28 valence-electron basis set of VDZ[30] quality was chosen for tellurium. For compound **1** the basis sets for H (3-1p1G), N (6-21G*) were taken from the CRYSTAL website,[31] and for Mn the recently developed pob-TZVP basis was used.[32] For compound **2** the iron basis set is pob-TZVP[32] and for H 3-1p1G,[31] N 6-31d1G.[31] For **3** the zinc basis is 86-411d41G, the H basis is 5-11G*, and the N basis is 6-21G*.[31] The Monkhorst−Pack grid was set to 4 × 4 × 4; the integral tolerance parameters were set to 7 7 7 7 14.[28]

The magnetic structure was investigated with unrestricted Kohn−Sham (UKS) calculations with all functionals mentioned above. Geometry relaxation in the case of the Mn compound and single point calculations of the Fe compound in both the high- and low-spin state have shown that the high-spin state is energetically preferred. This is in accordance with ligand field theory as ammonia is a weak ligand.

A Mulliken Population Analysis (MPA) was used to investigate the electronic structure of the compounds in terms of atomic charges and bond orders calculated as overlap population (OP). In the case of manganese(II) polytelluride **1** the MPA is not fully in accordance with the basic valence rules, but indeed the negative charge is much more localized on Te1 (−0.58) and Te4 (−0.59) compared to Te2 (−0.18) and Te3 (−0.33). Taking into account that the OP between Te4 and Te1 is only 0.01, whereas the OP between, e.g., Te1 and Te2 is about 0.26, the assumption can be made that the Te_4^{2-} units are rather isolated and do not interact by a chemical bond between Te4 and Te1, as anticipated.

In the case of iron(II) tetratelluride **2** the localization of the negative charge is less pronounced. Again, the terminal Te1 and Te4 atoms carry the highest charge (Te1 −0.39, Te4 −0.61), but the difference to the other tellurium atoms (Te2 −0.27, Te3 −0.43) is smaller than in the case of the manganese(II) compound. In addition the OP between Te3 and Te4 and between Te4 and Te1 is similar (Te3−Te4 0.05, Te4−Te1 0.07). We conclude that the tetratelluride units are connected via an at least partly covalent Te4−Te1 interaction that also weakens the Te3−Te4 bond.

In zinc(II) polytelluride **3** the negative charge is to a large extent localized on Te1 (−0.45), Te7 (−0.32), and Te8 (−0.40). Te4 is almost neutral, whereas the charge on Te2, Te3, Te5, and Te6 varies from −0.12 to −0.22. This indicates the presence of two Te_7 anionic chains connected by Te8. The number of possible interactions between the tellurium atoms is much larger than in the other compounds. From all the possibilities discussed in the Experimental Section, only one interaction could be identified using the OP. Only the Te7−Te8 (and Te7′−Te8) pairs showed a non-negligible OP of 0.09. The other OPs (Te4−Te8 0.03, Te2−Te2′ 0.00) are too small to be interpretable as covalent interactions. This is in accordance with the above finding based on the MPA.

Band structure calculations were performed in order to reveal the conducting or insulating nature of the compounds. In all three cases an insulating behavior was found with an indirect fundamental band gap. While the band gap for the manganese(II) compound **1** was at about 1.9 eV, the iron(II) telluride **2** had a band gap of only 1.6 eV. The slightly smaller electronic band gap indicates a tendency to charge delocalization which is in agreement with the observation based on the MPA that $[Mn(NH_3)_6]Te_4$ has rather distinct telluride units while the Te_4^{2-} chains in the iron(II) tetratelluride are interacting via (weak) bonds. Also, the zinc(II) telluride **3** turned out to be an insulator with an indirect fundamental band gap of 1.4 eV and a direct band gap of 1.54 eV at Γ point. That this band gap is smaller than in the cases of the Te_4^{2-} compounds is easily explained, as the electrons are delocalized over 7, or, taking the possible connection into account, 15 tellurium atoms. The absolute value is in reasonable agreement with the measured activation energy of 1.2 eV (*vide supra*). The calculated band structure for the zinc(II) compound is shown in Figure 4.

In order to further analyze the chemical bonding in the compounds, we calculated the total electronic density. For better visualization, the electronic density was projected on planes containing Te−Te or Te−H bonds.

In the manganese(II) telluride **1** the electron density is larger between Te3 and Te4 than between Te4 and Te1 as can be seen from Figure 5a. The density ranges from 0.1 to 0.0001 e/au^3 in a linear scale. In the density map a bonding interaction between Te3 and Te4 can also be seen, as the density increases

dx.doi.org/10.1021/ic302503u | *Inorg. Chem.* 2013, 52, 8327−8333

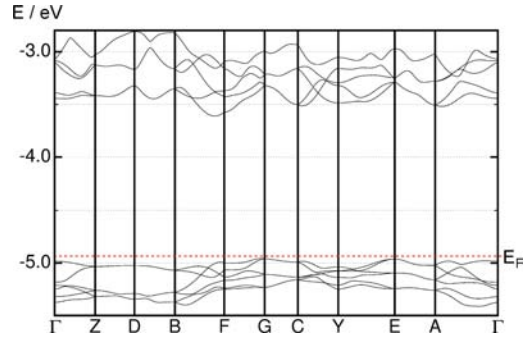

Figure 4. Calculated band structure (PW1PW) of $[Zn(NH_3)_4]Te_{15}$ in the HOCO–LUCO region.

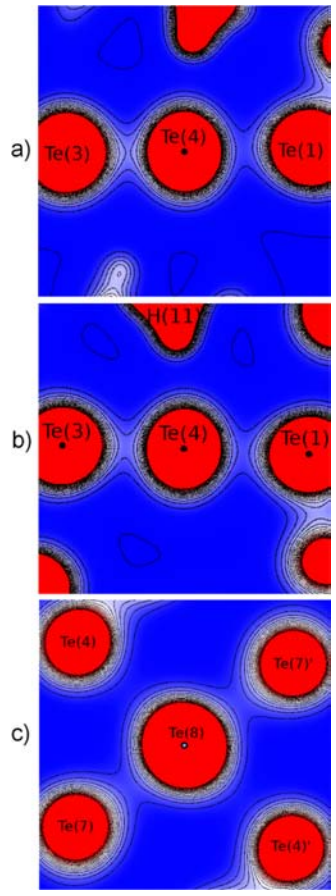

Figure 5. Electron density maps (calculated with PW1PW) of (a) $[Mn(NH_3)_6]NH_3$, (b) $[Fe(NH_3)_6]Te_4{\cdot}NH_3$, and (c) $[Zn(NH_3)_4]Te_{15}$; the numbering of the Te atoms corresponds that of to Figures 1–3. Regions of high density are shown in red (0.1 e/au^3), blue indicates a small density (0.0001 e/au^3), and white corresponds to a value of 0.05 e/au^3.

between the two nuclei. Since the electron density of Te4 does not show significant polarization in the direction of H11, the N–H···Te hydrogen bonding effects in the structure are small.

In the case of the iron(II) telluride **2** the difference in the electron density between Te3–Te4 and Te4–Te1 is much smaller than in the manganese(II) case. This similarity of the binding is in accordance with the previous analyses based on MPA and band structure. Similar to compound **1**, the polarization of Te4 toward H11 is not very pronounced indicating only weak hydrogen bonding.

The electron density maps for the zinc(II) telluride **3** show only interactions between Te7 and Te8. All other interactions between Te4–Te8, Te2–Te2′, and the possible hydrogen bonds are not significant. Due to the fact that Te8 is positioned in an inversion center, the interactions to Te7 and Te7′ are identical.

However, the electron density is smaller than between other neighboring tellurium atoms in the Te_7 chains.

CONCLUSIONS

Low temperature solvothermal synthesis in liquid ammonia turned out to be a very promising way toward novel polyanionic compounds. As a key advantage, the method allows for gentle experimental conditions with heating only up to 50 °C. Large structural blocks of the tellurium element structure are preserved from thermal desintegration during the synthesis. Additionally, the method is experimentally simple. Definite, crystalline, and pure phases of novel 3d metal polytellurides $[Mn(NH_3)_6]Te_4$ (**1**), $[Fe(NH_3)_6]Te_4{\cdot}NH_3$ (**2**), and $[Zn(NH_3)_4]_2Te_{15}$ (**3**) were obtained and crystallographically investigated. According to our knowledge, **3** represents the first example of a Te_{15}^{4-} anion and is found to behave as a small-gap semiconductor. All three compounds show the large variability of Te–Te covalent and noncovalent bonding interactions, which is typical for tellurium-rich tellurides. Besides the normal Te–Te bonds (Te–Te < 3.0 Å), Te–Te distances up to 3.8 Å correspond to weak bonding interactions. Large variability of these secondary interactions in **1**, **2**, and **3** causes high dimensionality of the polyanionic networks. A theoretical bonding analysis based on the Mulliken Population Analysis of the wave function obtained from periodic hybrid density functional calculations reveals the presence of isolated Te_4^{2-} chains in **1**, weakly interconnected Te_4^{2-} chains in **2**, and anionic Te_7 chains connected via Te8 in **3**. Hydrogen bonds are expected to play only a minor role in all three compounds.

ASSOCIATED CONTENT

Supporting Information

Thermal ellipsoid plots of all cationic ammine complexes, TG-DTA curves for **3**, and plots of electrical resistivity vs temperature for **3**. This material is available free of charge via the Internet at http://pubs.acs.org.

AUTHOR INFORMATION

Corresponding Author

*E-mail: j.beck@uni-bonn.de.

Notes

The authors declare no competing financial interest.

ACKNOWLEDGMENTS

We gratefully acknowledge the contributions of Dr. J. Daniels and A. Pelka, Institute for Inorganic Chemistry, University of Bonn, for the diffraction data collections, K. Armbruster for the thermal analyses, N. Wagner for the conductivity measurements, A. Eich for EDX analyses, and B. Knopp and Dr. S. Rings for ICP measurements.

REFERENCES

(1) Böttcher, P. *Angew. Chem., Int. Ed.* **1988**, *27*, 759–864; *Angew. Chem.* **1988**, *100*, 781–794. Kanatzidis, M. G. *Angew. Chem., Int. Ed.* **1995**, *34*, 2109–2111; *Angew. Chem.* **1995**, *107*, 2281–2283.

Sheldrick, W. S.; Wachhold, M. *Angew. Chem., Int. Ed.* **1997**, *36*, 206−224; *Angew. Chem.* **1997**, *109*, 214−234. Papoian, G. A.; Hoffmann, R. *Angew. Chem., Int. Ed.* **2000**, *39*, 2408−2448; *Angew. Chem.* **2000**, *112*, 2500−2544. Zhang, Q.; Armatas, G.; Kanatzidis, M. G. *Inorg. Chem.* **2009**, *48*, 8665−8667. Zhang, Q.; Malliakas, C. D.; Kanatzidis, M. G. *Inorg. Chem.* **2009**, *48*, 10910−10912. Graf, C.; Assoud, A.; Mayasree, O.; Kleinke, H. *Molecules* **2009**, *14*, 3115−3131.

(2) Lange, S.; Nilges, T. *Chem. Mater.* **2006**, *18*, 2538−2544.

(3) Yamada, N.; Wuttig, M. *Nat. Mater.* **2007**, *6*, 824−832. Kim, C.; Kang, D.; Lee, T.-Y.; Kim, K. H. P.; Kang, Y.-S. *Appl. Phys. Lett.* **2009**, *94*, 193504.

(4) Lowhorn, N. D.; Tritt, T. M.; Abbott, E. E.; Kolis, J. W. *Appl. Phys. Lett.* **2006**, *88*, 022101. Sootsman, J. R.; Kong, H.; Uher, C.; D'Angelo, J. J.; Wu, C.-I.; Hogan, T. P.; Caillat, T.; Kanatzidis, M. G. *Angew. Chem., Int. Ed.* **2008**, *47*, 8618−8622; *Angew. Chem.* **2008**, *120*, 8746−8750. Xu, H.; Kleinke, K. M.; Holgate, T.; Zhang, H.; Su, Z.; Tritt, T. M.; Kleinke, H. *J. Appl. Phys.* **2009**, *105*, 053703.

(5) Smith, D. M.; Ibers, J. A. *Coord. Chem. Rev.* **2000**, *200*−*202*, 187−205.

(6) Henshaw, G.; Parkin, I. P.; Shaw, G. *Chem. Commun.* **1996**, 1095−1096. Hector, A. L.; Henshaw, G.; Parkin, I. P.; Shaw, G. A. *Main Group Chem.* **1996**, *1*, 183−187. Henshaw, G.; Parkin, I. P.; Shaw, G. *J. Mater. Sci. Lett.* **1996**, *15*, 1741−1742. Henshaw, G.; Parkin, I. P.; Shaw, G. A. *J. Chem. Soc., Dalton Trans.* **1997**, 231−236.

(7) Sheldrick, G. M. *SHELXS97, Program for Crystal Structure Solution*; University of Göttingen: Göttingen, Germany, 1997.

(8) Sheldrick, G. M. *SHELXL97, Program for Crystal Structure Refinement*; University of Göttingen: Göttingen, Germany, 1997.

(9) Zhen Chen, R.-J.; Wang, X.-Y.; Huang, J. L. *Acta Crystallogr.* **2000**, *C56*, 1100−1103. Wendland, F.; Nather, C.; Bensch, W. *Z. Anorg. Allg. Chem.* **2000**, *626*, 456−461.

(10) Essmann, R.; Kreiner, G.; Niemann, A.; Rechenbach, D.; Schmieding, A.; Sichla, T.; Zachwieja, U.; Jacobs, H. *Z. Anorg. Allg. Chem.* **1996**, *622*, 1161−1166. Himmel, K.; Jansen, M. *Eur. J. Inorg. Chem.* **1998**, 1183−1186. Kysliak, O.; Beck, J. *Eur. J. Inorg. Chem.* **2013**, 124−133.

(11) Jacobs, H.; Bock, J.; Stüve, C. *J. Less-Common Met.* **1987**, *134*, 207−214. Essmann, R.; Kreiner, G.; Niemann, A.; Rechenbach, D.; Schmieding, A.; Sichla, T.; Zachwieja, U.; Jacobs, H. *Z. Anorg. Allg. Chem.* **1996**, *622*, 1161−1166.

(12) Sutherland, H. H.; Hogg, J. H. C.; Walton, P. D. *Acta Crystallogr., Sect. B* **1976**, *32*, 2539−2541.

(13) Doert, T.; Cardoso-Gil, R.; Böttcher, P. *Z. Anorg. Allg. Chem.* **1999**, *625*, 2160−2163.

(14) Valentine, D. Y.; Cavin, O. B.; Yakel, H. L., Jr. *Acta Crystallogr., Sect. B* **1977**, *33*, 1389−1396.

(15) Böttcher, P.; Kretschmann, U. *Z. Anorg. Allg. Chem.* **1982**, *491*, 39−46.

(16) Böttcher, P.; Kretschmann, U. *J. Less-Common Met.* **1983**, *95*, 81−91.

(17) Klinkhammer, K. W.; Böttcher, P. *Z. Naturforsch.* **1990**, *45b*, 141.

(18) Felser, C.; Finckh, E. W.; Kleinke, H.; Rocker, F.; Tremel, W. *J. Mater. Chem.* **1998**, *8*, 1787−1798.

(19) Dürichen, P.; Bensch, W. *Acta Crystallogr., Sect. C* **1997**, *53*, 267−269. Stöwe, K. *Solid State Sci.* **2003**, *5*, 765−769.

(20) Essmann, R.; Kreiner, G.; Niemann, A.; Rechenbach, D.; Schmieding, A.; Sichla, T.; Zachwieja, U.; Jacobs, H. *Z. Anorg. Allg. Chem.* **1996**, *622*, 1161−1166. Jacobs, H.; Bock, J.; Stüve, C. *J. Less-Common Met.* **1987**, *134*, 207−214. Himmel, K.; Jansen, M. *Eur. J. Inorg. Chem.* **1998**, 1183−1186. Bremm, S.; Meyer, G. *Z. Anorg. Allg. Chem.* **2003**, *629*, 1875−1880. Schoening, R. A.; Meyer, G. *Z. Anorg. Allg. Chem.* **1998**, *624*, 1389−1390. Schimek, G. L.; Kolis, J. W.; Long, G.-J. *Chem. Mater.* **1997**, *9*, 2776−2785.

(21) Böttcher, P.; Keller, R. *J. Less-Common Met.* **1985**, *109*, 311−321.

(22) McConnachie, J. M.; Ansari, M. A.; Bollinger, J. C.; Salm, R. J.; Ibers, J. A. *Inorg. Chem.* **1993**, *32*, 3201−3202. Smith, D. M.; Roof, L. C.; Ansari, M. A.; McConnachie, J. M.; Bollinger, J. C.; Pell, M. A.; Salm, R. J.; Ibers, J. A. *Inorg. Chem.* **1996**, *35*, 4999−5006. Müller, U.; Grebe, C.; Neumüller, B.; Schreiner, B.; Dehnicke, K. *Z. Anorg. Allg. Chem.* **1993**, *619*, 500−506.

(23) Assoud, A.; Derakhshan, S.; Soheilnia, N.; Kleinke, H. *Chem. Mater.* **2004**, *16*, 4193−4198.

(24) Xiaoying, H.; Roushan, M.; Emge, T. J.; Wenhua, B.; Thiagarajan, S.; Jen-Hao, C.; Ronggui, Y.; Jing, L. *Angew. Chem., Int. Ed.* **2009**, *48*, 7871−7874; *Angew. Chem.* **2009**, *121*, 8011−8014. Shreeve-Keyer, J. L.; Warren, C. J.; Dhingra, S. S.; Haushalter, R. C. *Polyhedron* **1997**, *16*, 1193−1199. Xiaoying, H.; Jing, L.; Huaxiang, F. *J. Am. Chem. Soc.* **2000**, *122*, 8789−8790. Jing, L.; Wenhua, B.; Wooseok, K.; Xiaoying, H.; Reddy, S. *J. Am. Chem. Soc.* **2007**, *129*, 14140−14141. Xiaoying, H.; Jing, L.; Yong, Z.; Mascarenhas, A. *J. Am. Chem. Soc.* **2003**, *125*, 7049−7055.

(25) Guggenberger, L. J. *Inorg. Chem.* **1969**, *8*, 2771−2774. Yamaguchi, T.; Lindqvist, O. *Acta Chem. Scand., Ser. A* **1981**, *35*, 811−814. Chrappova, J.; Schwendt, P.; Dudasova, D.; Tatiersky, J.; Marek, J. *Polyhedron* **2008**, *27*, 641−647.

(26) Bredow, T.; Gerson, A. R. *Phys. Rev. B* **2000**, *61*, 5194−5201.

(27) Beck, J.; Bredow, T.; Tjahjanto, R. T. *Z. Naturforsch.* **2009**, *64b*, 145−152.

(28) Dovesi, R.; Orlando, R.; Civalleri, B.; Roetti, C.; Saunders, V. R.; Zicovich-Wilson, C. M. *Z. Kristallogr.* **2005**, *220*, 571−573.

(29) George, P.; Glusker, J. P.; Markham, G. D.; Trachtman, M.; Bock, C. W. *Mol. Phys.* **2003**, *101*, 2451−2467.

(30) Peterson, K. A.; Figgen, D.; Goll, E.; Stoll, H.; Dolg, M. *J. Chem. Phys.* **2003**, *119*, 11113.

(31) http://www.crystal.unito.it/Basis_Sets/Ptable.html

(32) Peintinger, M. F.; Vilela Oliveira, D.; Bredow, T. *J. Comput. Chem.* **2013**, *34*, 451−459.